Neurorehabilitation and Neural Repair
http://nnr.sagepub.com/

Quantitative Kinematic Characterization of Reaching Impairments in Mice After a Stroke

Stefano Lai, Alessandro Panarese, Cristina Spalletti, Claudia Alia, Alessio Ghionzoli, Matteo Caleo and Silvestro Micera

Neurorehabil Neural Repair published online 16 October 2014
DOI: 10.1177/1545968314545174

The online version of this article can be found at:
http://nnr.sagepub.com/content/early/2014/10/08/1545968314545174

Published by:
SAGE
http://www.sagepublications.com

On behalf of:
ASNR AMERICAN SOCIETY OF NEUROREHABILITATION
American Society of Neurorehabilitation

Additional services and information for *Neurorehabilitation and Neural Repair* can be found at:

Email Alerts: http://nnr.sagepub.com/cgi/alerts

Subscriptions: http://nnr.sagepub.com/subscriptions

Reprints: http://www.sagepub.com/journalsReprints.nav

Permissions: http://www.sagepub.com/journalsPermissions.nav

>> OnlineFirst Version of Record - Oct 16, 2014

What is This?

Downloaded from nnr.sagepub.com at Scuola Superiore Sant'Anna on October 21, 2014

Neurorehabilitation and
Neural Repair
1–11
© The Author(s) 2014
Reprints and permissions:
sagepub.com/journalsPermissions.nav
DOI: 10.1177/1545968314545174
nnr.sagepub.com
SAGE

Quantitative Kinematic Characterization of Reaching Impairments in Mice After a Stroke

Stefano Lai, MSc[1,*], Alessandro Panarese, PhD[1,*], Cristina Spalletti, MSc[1,2], Claudia Alia, MSc[2,3], Alessio Ghionzoli, PhD[1], Matteo Caleo, PhD[1,2,†], and Silvestro Micera, PhD[1,4,†]

Abstract

Background and Objective. Kinematic analysis of reaching movements is increasingly used to evaluate upper extremity function after cerebrovascular insults in humans and has also been applied to rodent models. Such analyses can require time-consuming frame-by-frame inspections and are affected by the experimenter's bias. In this study, we introduce a semi-automated algorithm for tracking forepaw movements in mice. This methodology allows us to calculate several kinematic measures for the quantitative assessment of performance in a skilled reaching task before and after a focal cortical stroke. *Methods*. Mice were trained to reach for food pellets with their preferred paw until asymptotic performance was achieved. Photothrombosis was then applied to induce a focal ischemic injury in the motor cortex, contralateral to the trained limb. Mice were tested again once a week for 30 days. A high frame rate camera was used to record the movements of the paw, which was painted with a nontoxic dye. An algorithm was then applied off-line to track the trajectories and to compute kinematic measures for motor performance evaluation. *Results*. The tracking algorithm proved to be fast, accurate, and robust. A number of kinematic measures were identified as sensitive indicators of poststroke modifications. Based on end-point measures, ischemic mice appeared to improve their motor performance after 2 weeks. However, kinematic analysis revealed the persistence of specific trajectory adjustments up to 30 days poststroke, indicating the use of compensatory strategies. *Conclusions*. These results support the use of kinematic analysis in mice as a tool for both detection of poststroke functional impairments and tracking of motor improvements following rehabilitation. Similar studies could be performed in parallel with human studies to exploit the translational value of this skilled reaching analysis.

Keywords

ischemic stroke, mouse, skilled reaching, kinematics, video tracking

Introduction

Stroke can cause significant impairments in skilled forelimb movements such as reaching, grasping, and object manipulation. Upper-extremity function in poststroke patients is traditionally evaluated using clinical scales,[1] although kinematic analysis of movement is now increasingly used. For example, analysis of skilled reaching can provide objective and quantitative measures of motor performance and movement quality and can be used as a complementary tool to assess forelimb motor function.[2-6] Skilled reaching is a natural behavior in humans and requires no special training.

Translational research in poststroke rehabilitation often makes use of rodents to uncover the mechanisms underlying functional impairments and recovery. Skilled reaching can serve as a powerful model in this context.[7] In fact, although rodents display behavioral specializations quite different from humans, skilled reaching shares many similarities with the homologous behavior in humans. Assessment of skilled reaching performance can be done using a number of tasks in which the animal is trained to reach for food with the paw and to bring it to the mouth for eating.[8] Among these tasks, the single pellet reaching task is

[1]Scuola Superiore Sant'Anna, Pisa, Italy
[2]CNR, Neuroscience Institute, Pisa, Italy
[3]Scuola Normale Superiore, Pisa, Italy
[4]Ecole Polytechnique Federale de Lausanne (EPFL), Lausanne, Switzerland
[*]Equally contributing first authors, [†]Equally contributing senior scientists

Corresponding Author:
Alessandro Panarese, Translational Neural Engineering Laboratory, The BioRobotics Institute, Scuola Superiore Sant'Anna, Viale R. Piaggio 34, 56025 Pontedera, Pisa, Italy.
Email: a.panarese@sssup.it

Downloaded from nnr.sagepub.com at Scuola Superiore Sant'Anna on October 21, 2014

unique, as it permits multiple performance measurements.[9-16]

For both humans and rodents, limb movements can be documented using high-speed video recordings. Motor performance can then be assessed using both end-point measures of success and failure and kinematic measures of movement execution. Previous work[17] has shown that biomechanical markers can be fitted to rat hindlimbs, and movement kinematics can be automatically reconstructed (optical tracking). To our knowledge, this approach has never been used to study reaching movements. Moreover, the use of markers presents major difficulties in mice, as markers may be too bulky. Alternatively, video-based tracking methods can be employed.[9,10] These methods typically require time consuming frame-by-frame video analyses to manually digitize the coordinates of a specific target, for example, the mouse paw, in the background scene. Automatic digitizing algorithms exist, but their use is robust only when the target has a fixed shape and a high contrast with respect to the background. Unfortunately, this is rarely the case when tracking forelimb movements in mice.

Previous studies using rats have examined kinematic variables as measures of poststroke impairment and recovery, both qualitatively[9,10,12-16] and quantitatively.[18] These studies have been able to discern several parallels with reports in human subjects, such as the use of poststroke compensatory strategies and the production of more irregular movement patterns.[2-6,19-21] At the same time, only a limited number of investigations have involved mice,[7,11] in part due to the aforementioned difficulties of video-tracking methods. We have developed a semiautomated algorithm for tracking paw movements in mice during a skilled reaching task, without markers attached to the skin. Both the accuracy and precision of trajectory tracking were carefully tested. Later, the tool was applied to study reaching impairments after the induction of a focal ischemic stroke in the motor cortex. Paw trajectories were extracted off-line with limited inputs from the experimenter. Movement kinematics were then analyzed to assess differences in motor performance before and after stroke with a set of parameters chosen to facilitate future translational studies.

Methods

Development of the Apparatus

Mice were trained to perform a skilled reaching task in a testing chamber (TC; 13.5 × 5 × 9 cm) housed into a U-shaped plastic case (30 × 20 × 21 cm). The TC was made of black plastic (Delrin, Du Pont, Wilmington, DE) except for the frontal, bottom and lateral sides, which were made of Plexiglas (5 × 4.7 × 5 cm). The front wall of the TC had a small rectangular aperture (0.5 × 1.3 cm) 3 mm from the floor. During the task, the paw passed through the aperture to reach for a food pellet, placed in a slot 8 mm distant from the aperture. Below the transparent floor, a 45°-tilted mirror (6 × 3.7 cm) enabled the experimenter to view the animal from the bottom (Figure 1A).

A photo-detector, placed on the top of the TC, was aligned with a photo-diode placed under the slot containing the pellet, such that whenever the animal grasped the pellet, the photocell switched a red LED (*Feedback LED*) on. Reaching and grasping movements were recorded at 120 frames/s by a digital video camera (Hero 3, GO-Pro, San Mateo, CA), placed on a fixed support 13 cm from the TC. The camera was equipped with a macro lens (10×) and a Blurfix adapter to correct optical distortions in the acquired images. Appropriate lighting conditions were guaranteed by a cold-light source (CL 6000, ZEISS, Oberkochen, Germany). Before testing, both the palm and the back of the forepaw were painted with a green nontoxic dye (Stabilo Boss, Stabilo, Heroldsberg, Germany), which dried in a few minutes (Figure 1B).

Algorithm and Interfaces for Off-Line Analysis

Reconstruction of paw trajectories was performed off-line by a semiautomated algorithm based on color contrast analysis. The algorithm only required limited inputs from the experimenter, who interacted via a graphical user interface (GUI, Figure 1B). Both the tracking algorithm and the GUI were programmed in Matlab (MathWorks, Natick, MA).

The tracking process consisted of 3 distinct phases. In phase (i), the algorithm synchronized the recorded video and the photocell signal, which were acquired independently. Based on the switching times of the photocell, the video was segmented into short clips, each of which demonstrated a grasping attempt by the mouse. To discard clips not related to pellet grasping (e.g., the photocell switched because the experimenter was handling the pellet), the algorithm checked for the presence of the pellet in its slot in selected frames before each switch activation by asking the user to locate the pellet in the first frame via the GUI.

Before extracting the paw trajectory, the algorithm asked the user to select a part of the green area denoting the paw (*Paw area*) in a few ($n < 5$) initial frames. The algorithm used these pixels to define 3 average values (μ_k), and the corresponding confidence intervals (*gCIs*), of each RGB component of the green dye ($k = 1$, red; $k = 2$, green; $k = 3$, blue), which would be used in phase (ii) to locate the paw in all of the subsequent frames.

In phase (ii), the x (anteroposterior), y (dorsoventral), and z (mediolateral) Cartesian coordinates of paw position were automatically extracted from each frame of a grasping attempt. Trajectories were composed of 321 points (ie, they described ~3-second long paw movement), and the central point ($i = 160$) corresponded to the switching time of the photocell. To extract paw position from a frame, the

Downloaded from nnr.sagepub.com at Scuola Superiore Sant'Anna on October 21, 2014

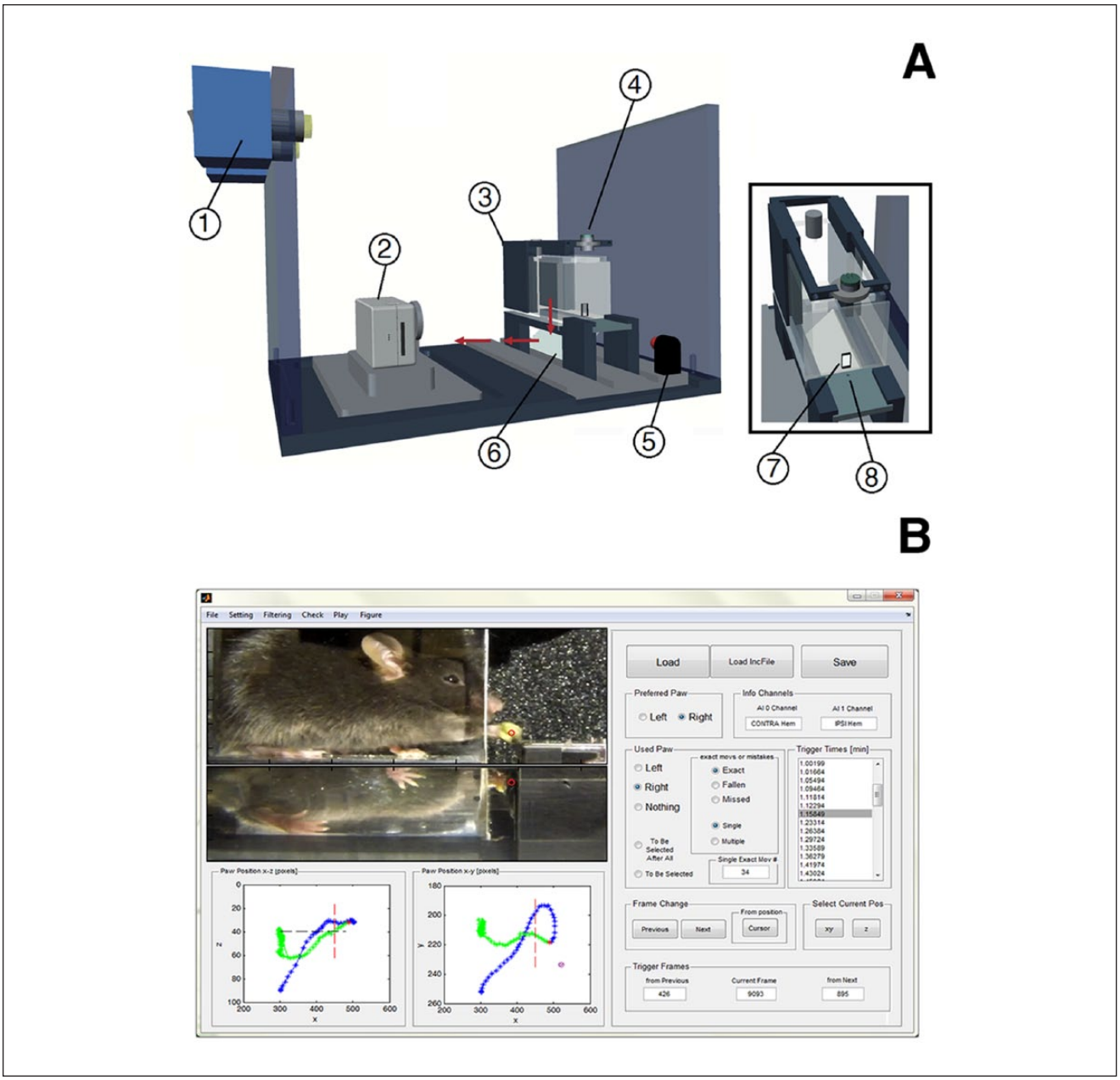

Figure 1. Experimental setup. (A) Schematic representation of the apparatus, which consists of a cold-light source (1), a digital video camera (2), a testing chamber (3), a photocell (4), a red LED, (5) and a mirror (6). The testing chamber has a rectangular aperture in the front wall (7), through which the paw reaches for a food pellet placed in a slot (8). (B) Snapshot of the graphical user interface for off-line trajectory tracking. The left part displays selected frames of the recorded video (top) and the reconstructed trajectory in the sagittal (*x, y*) and coronal (*x, z*) planes (bottom). The right part allows the experimenter to select a specific trial, to navigate across frames and to mark key features.

algorithm searched for green spots within the image. The RGB color components of all of the pixels in the frame were compared with the *gCIs*, and the groups of pixels with color levels included in the *gCIs* were selected as possible regions of interest (pROIs). In case of multiple pROIs, the algorithm looked for the largest region with the most similar colors with respect to the *Paw Area* selected by the user. A metric *m* assessing both spatial extent (*Area*) and color levels (d_{Col}) was computed for each pROI:

$$m = \frac{Area(pROI)}{d_{Col}}.$$

Downloaded from nnr.sagepub.com at Scuola Superiore Sant'Anna on October 21, 2014

The parameter d_{Col} is defined as

$$d_{Col} = \sum_{k=1}^{3} abs\left(\frac{1}{n}\sum_{i=1}^{n} X_{i,k} - \mu_k\right)$$

and weights the difference between the RGB components of all n pixels in the pROI, $X_{i,k}$, and the central values of the *gCIs,* μ_k. The pROI with the largest value of m was chosen as the best candidate among the pROIs, and the coordinates of its centroid were selected as the new paw position. Although not used in the following analyses, the z-coordinate of the paw could also be detected by applying a similar procedure to the plane (x, z). Once the paw position was extracted for all 321 frames, a third-order Savitzky–Golay Filter was applied to smooth the trajectory.

In phase (iii), the user had to perform a quick review of the extracted trajectories, and assign them to 3 categories: *exact*, that is, a reach and grasp movement ending with pellet eating; *missed*, if the mouse reached for the pellet but missed it or knocked the food away; and *fallen*, if the animal dropped the pellet after grasping it.

Algorithm Testing Procedures

The accuracy and precision of trajectory tracking were evaluated by comparing automatically extracted trajectories (*aTs*) with curves manually extracted by a skilled experimenter (*mTs*). Reach and grasp movements from a single animal were analyzed before (n = 12) and after (m = 5) lesion. The experimenter derived the trajectory by manually inspecting each frame of the video recording for a given movement, and selecting the center point of the green region denoting the paw in the GUI in manual mode. The coordinates of the points in all 321 frames were then collected together to form the trajectory. To assess tracking accuracy and precision, the average difference and the root mean square errors (RMSEs) between *mTs* and *aTs* were computed.

During the task, the dye on the paw inevitably faded, potentially affecting tracking accuracy. Therefore, variations of the RMSE along a session were also analyzed to assess the robustness of tracking performance.

Animals and Experimental Protocol

All procedures were performed according to the guidelines of the Italian Ministry of Health for the care and maintenance of laboratory animals (law 116/92), and in compliance with the EU Council Directive n. 86/609. Thirteen male C57BL/6J mice were included in the study (22-27 g, age 8-10 weeks). Prior to the experiment, animals were gradually habituated to the TC. They were trained 5 days a week for at least 2 weeks to reach and grasp small food pellets (10 mg chocolate flavored Purified Rodent Tablet 5TUL, TestDiet, St. Louis, MO). Mice were food deprived overnight before testing, which was always performed at the same time in the morning. On learning the task, mice started the experimental sessions, each lasting for 5 minutes.

End-point measures of reaching performance and kinematic parameters computed from trajectories were collected in n ≥ 5 daily sessions before treatment. All mice were also tested on 2 behavioral tests, the Gridwalk test and the Schallert cylinder, to acquire a baseline performance of sensorimotor coordination and preference of forelimb use. Animals were then assigned to 2 groups: *ischemic* (n = 7) and *sham* (n = 6). Ischemic animals underwent Rose Bengal–induced photothrombosis, causing a focal ischemic injury in the motor cortex.[22] Rose Bengal was injected intraperitoneally (0.2 mL of a 10 mg/mL solution), and the brain was illuminated through the intact skull for 15 minutes using a cold light source (CL 6000, ZEISS, Oberkochen, Germany) attached to a 20× objective that was positioned 0.5 mm anterior and 1.75 mm lateral from bregma. Sham animals received Rose Bengal intraperitoneally but with no cortical illumination. All animals were then tested on the behavioral tests and the skilled reaching task two days after treatment and once a week for the following 5 weeks.

End-Points Measures and Behavioral Analysis

A traditional end-point analysis of the reaching task[10,11] was performed to quantify the percentage of exact reaching movements, defined as

$$Exact\,Movs\,\% = 100 * \frac{\#\,exact\,retrievals}{\#\,total\,reaching\,attempts}$$

where the total number of reaching attempts were those detected by the photocell during the 5-minute testing period (see section Algorithm and Interfaces for Off-Line Analysis). Within each test session, the total number of reaching attempts depended both on the subject and the time point (before or after stroke). Before lesion, mice performed 54 ± 3 trials (mean ± SEM), while 2 days after stroke this value decreased to 30 ± 4 trials. Thirty days after stroke, the average number of total trials increased to 41 ± 5.

The Schallert cylinder is widely used to test the level of preference for use of the nonimpaired forelimb after unilateral cortical injury.[23] Animals were placed in a transparent Plexiglas cylinder (8 cm diameter, 15 cm height), closed at the top and fixed to a transparent base. A camera (SMX-F50BP/EDC, Samsung, Seoul, South Korea) was placed below the cylinder in order to record the animal from below during the exploration of the vertical walls. All mice were tested in 5-minute sessions. To quantify forelimb-use asymmetry, the asymmetry index was computed

Downloaded from nnr.sagepub.com at Scuola Superiore Sant'Anna on October 21, 2014

$$Asymmetry\,Index = \left(\frac{C_{ipsi}}{C_{ipsi}+C_{contra}}\right)*100 - \left(\frac{C_{contra}}{C_{ipsi}+C_{contra}}\right)*100$$

where C_{ipsi} and C_{contra} refer, respectively, to the number of contacts performed with the limb ipsilateral and contralateral to the lesioned hemisphere.

During the Gridwalk test, the animal was allowed to walk freely on an elevated grid of 32 × 20 × 52 cm, with 11 × 11 mm openings.[24,25] A mirror was placed under the grid to facilitate observation of the task by the experimenter. The task was recorded using a camera placed in front of the grid. Animals were given 5 minutes to walk on the elevated surface. The video recordings were analyzed off-line through a custom-designed GUI implemented in Matlab[26] to assess the animal's foot-faults, that is, steps not providing body support, with the foot falling in a grid hole. Foot-faults were counted for the preferred forelimb and compared to the total steps performed with that limb. Then, the foot-fault % was calculated as follows:

$$Foot\,Faults\% = 100 * \frac{\#\,foot\,faults}{\#\,correct\,steps + \#\,foot\,faults}$$

Kinematic Analysis

To ensure consistency, only trajectories from successful (*exact*) trials were considered. Paw positions from non-informative video frames (ie, those preceding the beginning of the movement or following task completion) were automatically removed from the trajectory. Based on previous studies on the kinematics of poststroke upper limb movements in humans,[2-6,19-21] several kinematic measures were computed to detect overall and local modifications of paw movements before versus after stroke (Figure 2).

Overall changes include variations in the length of the end-point trajectory (*ArcLen*), the area enclosed by the curve (*AUC*), the average tangential velocity (*Mean Speed*) and the movement smoothness, quantified by the number of peaks in the tangential velocity profile (*Smoothness*).

Local curve modifications take into account changes in the maximum height reached by the paw during the movement (*Height*), the curvature of the trajectory when the paw approaches the pellet (*CurvRadius*), the fraction of the total trials during which a dragging movement occurs (*Dragging*) and the duration of dragging (*tDrag*). Dragging was automatically detected when the height of the paw during the retraction phase and on crossing the aperture in the front wall remained below a threshold, *hT*, for at least a fixed time period, *tT*. The threshold *hT* was set at 3 mm from the floor of the testing chamber (ie, corresponding with the bottom side of the aperture in the wall), while *tT* was set as 2 * *tCA*, where *tCA* was the mean time required to retract the paw from the pellet slot to the aperture for each animal. This allowed us to take into account the inter-individual variability in speed of the retraction movement.

Tracking precision may significantly affect how robustly the kinematic parameters are estimated from the trajectories because noise on extracted paw position, $\Delta\boldsymbol{x}$, inevitably spreads into other parameters: $p(\boldsymbol{x} \pm \Delta\boldsymbol{x}) \approx p \pm \sigma_p$. A simulation study was thus carried out to ascertain whether tracking precision significantly contributed to the variations on the kinematic parameters, Δp, observed within and across the experimental sessions, that is, whether $\sigma_p \approx \Delta p$. Ten trajectories extracted automatically by the algorithm (*aTs*) were randomly selected from a single experimental session. For each trajectory, $n = 1000$ curves (*sim-aT*s) were simulated such that all points in *aT*, $\boldsymbol{P_i} = (x_i, y_i, z_i)$, were replaced by new points $\hat{\boldsymbol{P}}_{\boldsymbol{i}}$ with coordinates: $\hat{x}_i = x_i + \varepsilon_x$, $\hat{y}_i = y_i + \varepsilon_y$, and $\hat{z}_i = z_i + \varepsilon_z$. The values for ε_x, ε_y, and ε_z were randomly drawn from uniform distributions on the interval $[-TrP\ TrP]$, where *TrP* was the estimated precision of the tracking algorithm over the 3 axes (see section "Algorithm Testing Procedures"). Finally, the kinematic parameters were recalculated on the *sim-aT*s in order to evaluate the intrinsic variability of parameter estimates, σ_P, as

$$\sigma_P = [\max_{sim-aTs}(p) - \min_{sim-aTs}(p)]/2$$

where $\max_{sim-aTs}(p)$ and $\min_{sim-aTs}(p)$ are, respectively, the maximum and minimum values for the parameter *p*, computed on all 1000 *sim-aTs*.

Tissue Processing and Immunostaining

At the end of the experiment, all animals were transcardially perfused with 4% paraformaldehyde. Brains were cut using a sliding microtome (Leica, Wetzlar, Germany) to obtain 50-µm thick coronal sections that were used for immunostaining of NeuN (anti-NeuN guinea pig antibody 1:1000, Millipore, Billerica, MA) and glial fibrillary acidic protein (GFAP, Rabbit Polyclonal, DAKO, Glostrup, Denmark). To quantify the lesion volume, 1 out of every 6 sections was stained with Hoechst 33258 (Sigma-Aldrich, St. Louis, MO). The ischemic region was contoured using a 10× objective and its area measured by Stereo Investigator software (MBF Bioscience, Williston, VT). The lesion volume for each animal was calculated by summing up all damage areas and multiplying the number by section thickness and by 6 (the spacing factor). A total infarction volume in mm^3 is given as the mean ± standard error of all analyzed animals.

Downloaded from nnr.sagepub.com at Scuola Superiore Sant'Anna on October 21, 2014

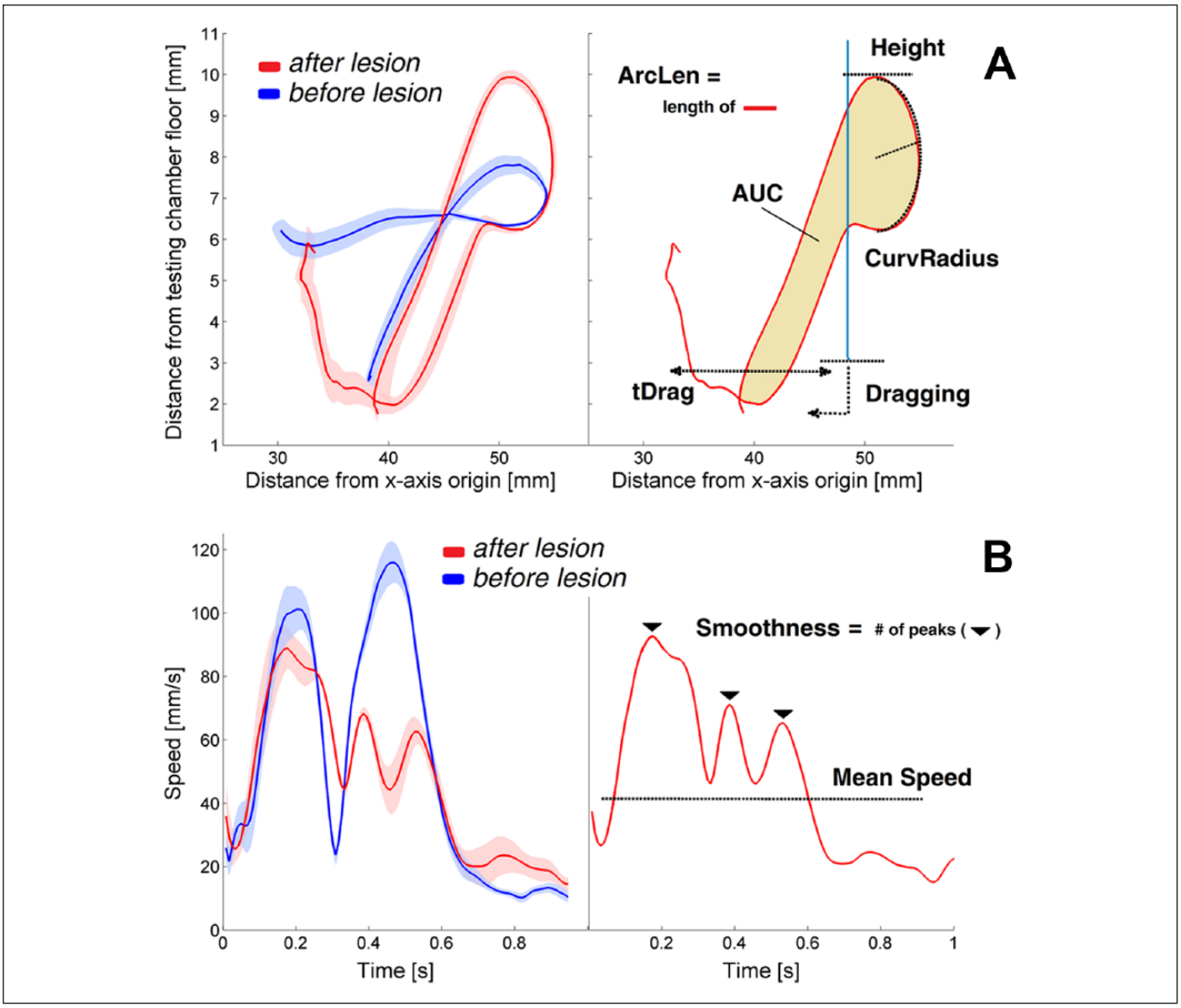

Figure 2. Reaching trajectories and extracted kinematic parameters. (A) On the left, average trajectories (solid lines) recorded before (blue, n = 16) and after stroke (red, n = 11) during 2 experimental sessions of the same mouse. The standard error is represented by the shaded region. On the right, kinematic parameters computed from the trajectories. The vertical blue line represents the aperture in the front wall. (B) On the left, average profiles and standard errors of tangential velocities measured before (blue, n = 16) and after stroke (red, n = 11). On the right, kinematic parameters computed from the speed curves.

Statistical Analysis

Data were analyzed with R, a free language and environment for statistical computing.[27] To evaluate differences between pre- and posttreatment performance in the pellet reaching task, the Gridwalk test, and the Schallert cylinder task, a Kruskal–Wallis test was used, followed by Tukey's post hoc analysis. For the pellet grasping task, posttreatment values were normalized to baseline prior to testing. To assess variations between baseline and posttreatment values of the kinematic parameters, all values were normalized to baseline and a Kruskal–Wallis test was used, followed by Tukey's post hoc analysis. Differences were considered significant at $P < .05$.

Results

Characterization of the Apparatus

Tracking Accuracy and Precision. Systematic errors between manually (*mT*) and automatically (*aT*) extracted trajectories (*Accuracy*) were, on average, 0.01, 0.078, and 0.028 mm for the *x, y*, and *z* axes, respectively, and did not significantly differ from zero. Tracking precision (*TrP*) along the

Downloaded from nnr.sagepub.com at Scuola Superiore Sant'Anna on October 21, 2014

x, y, and *z* axes was, respectively, 0.19, 0.18, and 0.19 mm. The algorithm also proved to be robust over sessions, as a correlation analysis between *TrP* and the duration of daily sessions failed to show any significant linear (Pearson's correlation coefficient) or nonlinear (Spearman's rank correlation coefficient) statistical relationship.

Reliability of Kinematic Measures. All the measured kinematic parameters were only weakly affected by tracking precision. The estimated intrinsic variability, σ_P, was 1.12 mm for *ArcLen*, 2.41 mm^2 for *AUC*, 4.1 mm/s for *Mean Speed*, 0.6 peaks for *Smoothness*, 0.12 mm for *Height*, 0.02 mm for *CurvRadius*, 0.01 seconds for *tDrag*, whereas *Dragging* was not affected. All of these quantities represent a minimal percentage (~9%, on average) of the differences observed between baseline conditions and the first poststroke session (ie, because of lesion-induced modifications of movement kinematics).

Reduction of Computational Time. The tracking algorithm significantly reduced the time needed for trajectory extraction compared with a manual operator. The total computational time required by the algorithm was evaluated by considering the sum of the time spent to perform each of the three phases. The total time to analyze approximately 18 500 frames was nearly 90 minutes, much less than what a human operator would have spent (~25 hours) to perform the same analysis, assuming an average speed of 0.2 frames/s.

Assessment of Impairments After Stroke

Photothrombotic Lesion. The photothrombotic lesion was confined to the cortical area of the hemisphere contralateral to the trained forelimb. Immunohistochemical analysis showed a complete loss of neurons in the core of the lesion (loss of NeuN staining) and a substantial glial scar surrounding the lesion edges (GFAP staining; Figure 3A). The total infarction volume, measured in Hoechst-stained sections (Figure 3B), was 1.22 ± 0.57 mm^3.

End-Point Measurements. In ischemic animals, the percentage of exact movements significantly dropped in the first 2 weeks postlesion ($P < .05$), but significantly recovered afterward (Figure 4A, red bars), indicating an improvement of forelimb function for this task. In contrast, no variation was observed between pre- and posttreatment values in the control (sham) group (Figure 4A, blue bars).

Testing in both the Gridwalk test (Figure 4B) and the Schallert cylinder task (Figure 4C) confirmed that ischemic mice performed significantly worse after the lesion ($P < .001$). Interestingly, no significant recovery to baseline performance was observed in these tasks up to 30 days postsurgery, indicating that the enhancement of forelimb function revealed by the pellet reaching test was not directly

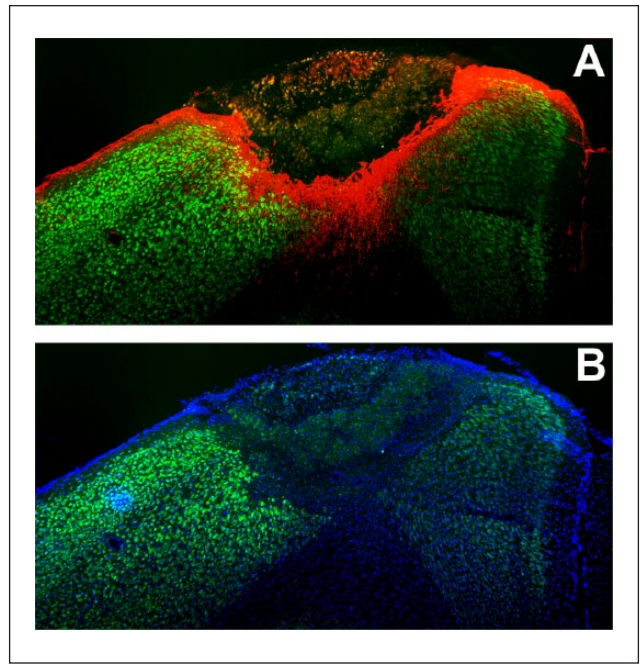

Figure 3. Stroke-induced brain damage. Representative coronal brain section showing the lesion and the perilesional area. (A) NeuN (green) and GFAP (red) immunostaining; (B) NeuN (green) and Hoechst (blue) labeling.

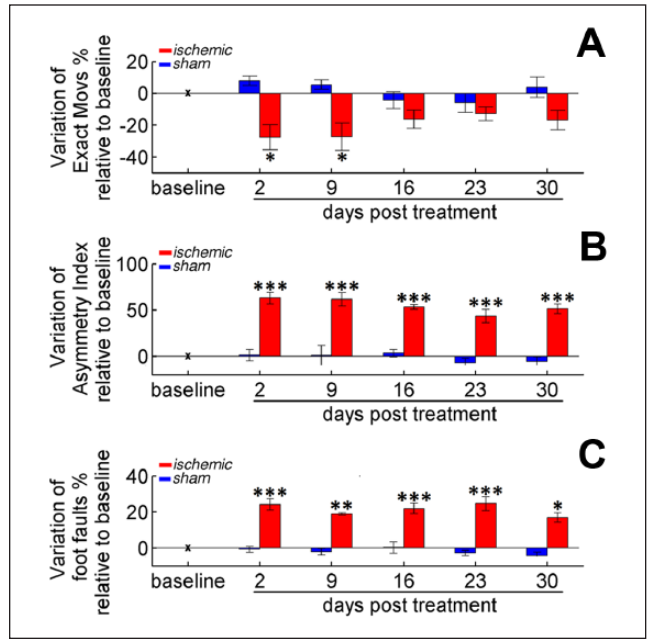

Figure 4. End-point measures for assessing forelimb impairments. (A) Variation of *% Exact Movs* in the pellet reaching task. (B) Changes in the *Asymmetry Index* in the Schallert cylinder. (C) Modifications in *% of Foot Faults* in the Gridwalk test. For all panels, bars refer to days 2, 9, 16, 23, and 30 after treatment: stroke (red) or sham (blue). Values are normalized by subtracting baselines (see Table 1), and plotted as the means ± standard error. Asterisks correspond to the following significance values: *$P < .05$, **$P < .01$, ***$P < .001$.

Downloaded from nnr.sagepub.com at Scuola Superiore Sant'Anna on October 21, 2014

Table 1. Values of the Kinematic Parameters at Baseline and the *P* Value of the Statistical Comparisons Between Measures at Baseline and at Day 2 Posttreatment.

	Baseline Values			*P* (Baseline vs Day 2 Posttreatment)	
Parameter	Q1	Q2	Q3	Stroke	Sham
ArcLen (mm)	42.42	47.09	53.58	10^{-7}	.34
AUC (mm^2)	8.17	13.48	21.08	10^{-8}	.99
Mean Speed (mm/s)	44.43	59.44	70.43	10^{-8}	.73
Smoothness (no. of peaks)	3	4	5	10^{-8}	.99
Height (mm)	7.09	7.95	8.79	10^{-8}	.83
CurvRadius (mm)	0.08	0.15	0.30	10^{-8}	.51
Dragging (%)	12	21	64	10^{-8}	.99
tDrag (s)	0	0	0.06	10^{-8}	.99

Abbreviations: Q1, first quartile; Q2, second quartile; Q3, third quartile; ArcLen, length of the end-point trajectory; AUC, area under the curve; CurvRadius, curvature of the trajectory when the paw approaches the pellet; tDrag, duration of dragging.

transferred to tasks in which the forelimb is nonspecifically employed.

Kinematic Parameters. After the habituation phase, mice were tested daily and their performance was video recorded. Baseline values of each kinematic parameter were computed based on pooled trajectories from the three sessions preceding treatment. Quartiles of the parameter values at baseline are reported in Table 1. We found that these measures varied considerably among animals, likely reflecting interindividual differences in grasping strategies.[28,29] Because we were primarily interested in highlighting differences in performance of individual animals before versus after stroke, we hereafter report values observed during post-stroke sessions as changes with respect to baseline.

Various kinematic parameters detected differences in reaching performance before versus after stroke. For the ischemic group, all parameters computed during the first poststroke session showed significant differences from baseline ($P < .001$; Figures 5 and 6). Movements performed by the *ischemic* group were longer (+8 mm, *ArcLen*), slower (−16 mm/s, *Mean Speed*), had an increased number of trajectory adjustments (+2.7 peaks, *Smoothness*) and spanned a broader workspace (+22 mm^2, *AUC*) than at baseline. When looking at local trajectory modifications, both the reaching and the retraction phases of the task were affected: Reaching movements were higher (+0.9 mm, *Height*), and mice approached the pellet with a larger curvature (+1.02 mm, *CurvRadius*) than at baseline. Moreover, dragging after pellet grasping occurred more frequently (+66%, *Dragging*) and lasted for a longer period of time (+0.48 s, *tDrag*) than at baseline.

For 4 parameters, *AUC, ArcLen, CurvRadius*, and *Height*, differences with respect to baseline values remained significant up to 30 days after lesion ($P < .001$), while *tDrag* and *Dragging* recovered to baseline after 3 and 4 weeks, respectively. *Mean Speed* and *Smoothness* yielded less reliable outcomes at weeks 2 to 5 because differences from baseline became comparable with intrinsic variations due to tracking precision (ie, $\Delta p \approx \sigma_p$; see section Reliability of Kinematic Measures).

Sham treatment did not significantly impact performance, and all of the parameter values remained stable throughout the observation period, except for *ArcLen* and *Height*, which showed small drifts at days 23 and 30 posttreatment (Figures 5 and 6). Taken together, these results reveal that stroke induces persistent (up to 30 days) kinematic modifications on reaching movements, whereas reaching success improves after 2 weeks (Figure 4). This improvement of motor performance observed using endpoint measures relies on the application of compensatory strategies rather than on restitution of the original movement patterns.

Discussion

The present study was aimed at designing a quantitative approach to characterize impairments in skilled reaching induced by a focal stroke in the mouse motor cortex. For the first time, kinematic modifications of reaching movements in the mouse have been described by a set of measures computed from paw trajectories extracted automatically rather than by manual frame-by-frame video analyses. Our findings demonstrate that, in the mouse model, key kinematic measures are sensitive to detect differences in performance before versus after stroke.

Reaching success by the forepaw contralateral to the lesion was impaired after stroke, and did not recover in the first 2 postsurgical weeks (Figure 4A). The photothrombotic lesion also caused distinct changes in forelimb preference (Schallert cylinder) and important deficits in sensory–motor coordination (Gridwalk test). From the third week on, the percentage of successful grasps showed a significant increase, indicating specific improvements in forelimb function. Nevertheless, performance on the Schallert cylinder and Gridwalk tests remained defective up to 30 days after surgery. This result is consistent with previous work in mice[11,30] and suggests that mechanisms underlying improvements in grasping control are—at least partially—independent from those contributing to the recovery of other behaviors (Figure 4B and C). However, it is also possible that an intensive training regimen is necessary to produce functional gains that extend to dissimilar, untrained tasks. For example, in rats with spinal cord lesions, daily training in the pellet reaching task leads to a small but detectable improvement in performance on the horizontal

Downloaded from nnr.sagepub.com at Scuola Superiore Sant'Anna on October 21, 2014

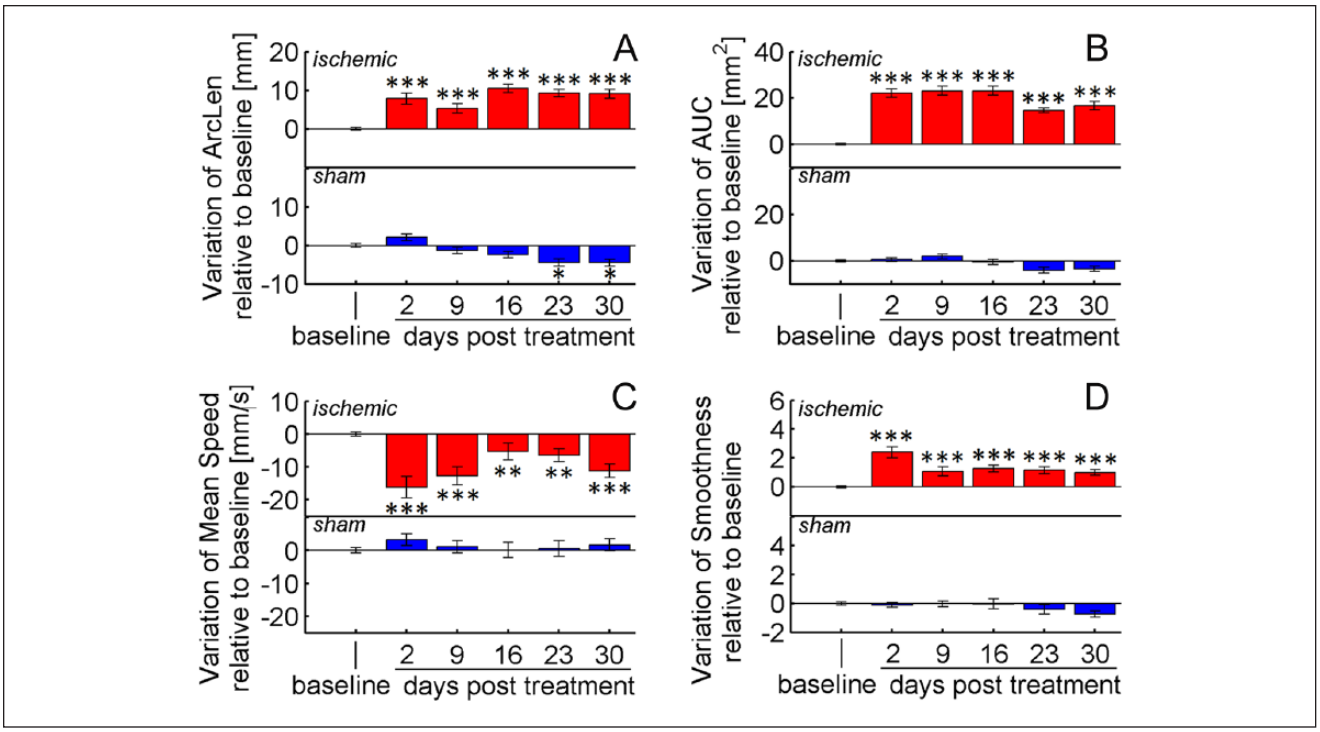

Figure 5. Overall kinematic modifications. Variations of (A) *ArcLen*, (B) *AUC*, (C) *Mean Speed*, and (D) *Smoothness* at 2, 9, 16, 23, and 30 days after treatment: stroke (red) or sham (blue). Values are normalized by subtracting baselines and plotted as the means ± standard error. Asterisks correspond to the following significance values: **P* < .05, ***P* < .01, ****P* < .001.

ladder test.[31] Concerning the neural mechanisms subserving functional recovery, Clarkson et al[30] recently found that early improvements in skilled reaching performance were associated with somatosensory remapping of perilesional areas of the mouse sensorimotor cortex. In addition, Nudo's group[32] has shown that gains in reaching performance can also be achieved by facilitating the restoration of cortico-cortical communication between spared, nonadjacent somatosensory and motor regions of the brain. Thus, early restoration of communication between somatosensory and motor brain regions seems to be the key to facilitate improvements in grasping control.

Rodent skilled reaching represents an ideal translational model and a powerful tool to generalize preclinical research to clinical conditions. In this work, kinematic modifications of successful reaching movements were analyzed by a semiautomated tool that proved to be accurate, precise and robust. Moreover, a significant reduction in the time required by a manual operator to perform a similar analysis was obtained. Previously, only qualitative kinematic modifications of reaching movements were assessed in a mouse model of stroke.[7,11] Although a detailed description of movement patterns was provided by the authors, including digit flexion or extension, this type of analysis is severely limited by interrater variability and by the need for time consuming frame-by-frame inspections of the filmed reaching movements. In contrast, the approach presented in this study is independent of an operator's expertise and provides objective and prompt measures of impairment. These are desirable features, especially for studies aimed at recording and analyzing multiple signals in parallel (eg, kinematic and neurophysiologic signals), or for rehabilitation protocols monitoring and controlling task practice to match task difficulty to the subjects' abilities.

Several parameters were computed from the extracted trajectories to describe both overall and local modifications of reaching movements. The analysis showed that these measures were quite stable over the observation period in unlesioned mice, with minor fluctuations in a few parameters (*ArcLen* and *Height*). In contrast, the kinematic parameters exhibited robust and consistent variations after stroke, demonstrating abnormal forepaw movements (Figures 5 and 6). Mice tended to move the paw higher than in baseline conditions when getting closer to the pellet, and approached the food with a different curvature. Moreover, the overall movements were significantly longer, slower, irregular and spanned a broader workspace. Finally, when retracting the paw toward the mouth to eat the pellet, dragging occurred more frequently and for a longer period of time. When compared to studies in humans,[2-6,19-21] important similarities were observed in the trajectories of the 2 species, captured

Downloaded from nnr.sagepub.com at Scuola Superiore Sant'Anna on October 21, 2014

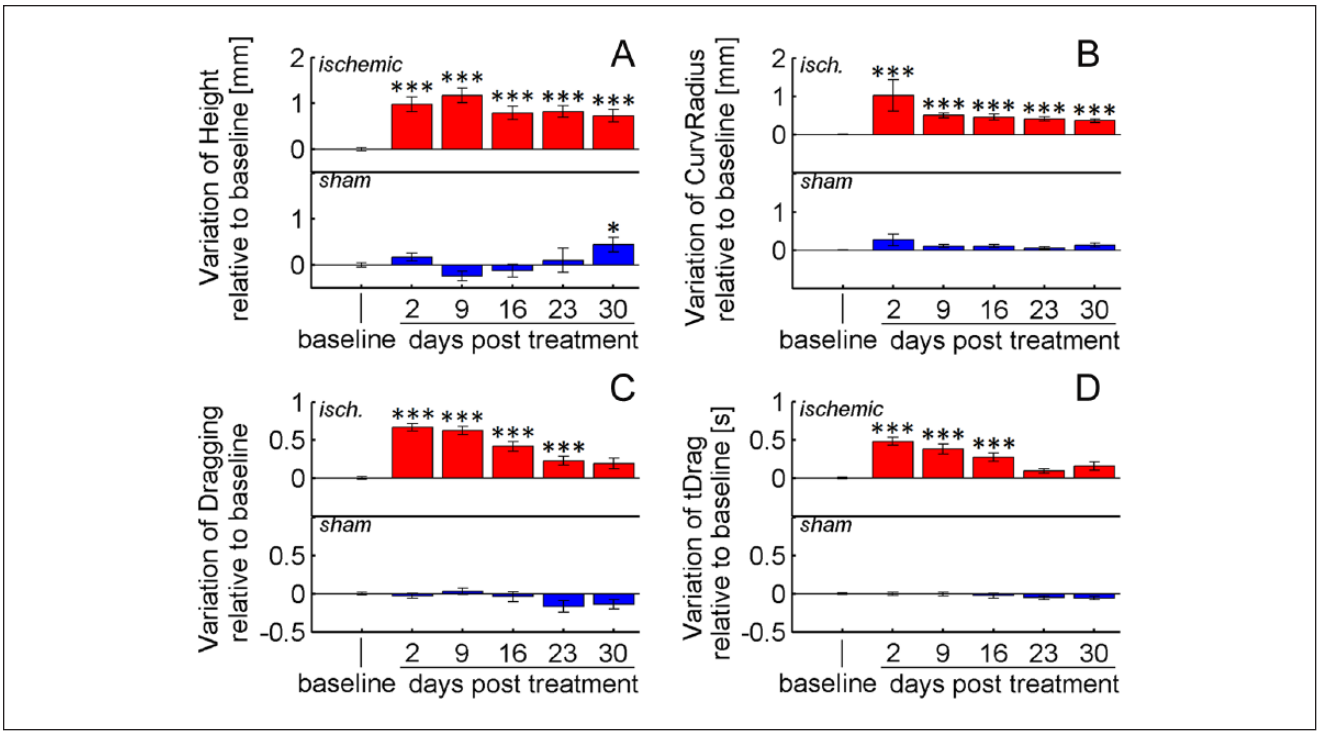

Figure 6. Local kinematic modifications. Variation of (A) *Height*, (B) *CurvRadius*, (C) *Dragging*, and (D) *tDrag* at 2, 9, 16, 23, and 30 days after treatment: stroke (red) or sham injection (blue). Values are normalized by subtracting baselines, and plotted as the means ± standard error. Asterisks correspond to the following significance values: **P* < .05, ***P* < .01, ****P* < .001.

by the parameters *ArcLen, Mean Speed*, and *Smoothness*: Poststroke reaching movements are longer, slower, and irregular. No comparison, however, was possible on the other parameters, which have never—to our knowledge—been investigated in humans. Nevertheless, they represent potentially interesting biomarkers of poststroke impairment and deserve to be tested in future rehabilitation protocols.

In conclusion, our results emphasize the utility of the mouse model and of kinematic analysis to assess functional impairments and, potentially, to track improvements in motor performance following stroke therapies that may ultimately be generalizable to patient populations.

Authors' Note

Authors Stefano Lai and Alessandro Panarese contributed equally to this study. Senior scientists Matteo Caleo and Silvestro Micera contributed equally to this study.

Declaration of Conflicting Interests

The author(s) declared no potential conflicts of interest with respect to the research, authorship, and/or publication of this article.

Funding

The author(s) disclosed receipt of the following financial support for the research, authorship, and/or publication of this article: This work was supported by the Fondazione Pisa.

References

1. Baker K, Cano SJ, Playford ED. Outcome measurement in stroke: a scale selection strategy. *Stroke*. 2011;42:1787-1794.
2. Cirstea MC, Levin MF. Compensatory strategies for reaching in stroke. *Brain*. 2005;123:940-953.
3. Subramanian SK, Yamanaka J, Chilingaryan G, Levin MF. Validity of movement pattern kinematics as measures of arm motor impairment poststroke. *Stroke*. 2010;41:2303-2308.
4. Alt Murphy M, Willén C, Sunnerhagen KS. Kinematic variables quantifying upper-extremity performance after stroke during reaching and drinking from a glass. *Neurorehabil Neural Repair*. 2011;25:71-80.
5. Alt Murphy M, Willén C, Sunnerhagen KS. Responsiveness of upper extremity kinematic measures and clinical improvement during the first three months after stroke. *Neurorehabil Neural Repair*. 2013;27:844-853.
6. van Dokkum L, Hauret I, Mottet D, Froger J, Métrot J, Laffont I. The contribution of kinematics in the assessment of upper limb motor recovery early after stroke. *Neurorehabil Neural Repair*. 2014;28:4-12.
7. Klein A, Sacrey LR, Whishaw IQ, Dunnett SB. The use of rodent skilled reaching as a translational model for investigating brain damage and disease. *Neurosci Biobehav Rev*. 2012;36:1030-1042.
8. Klein A, Dunnett SB. Analysis of skilled forelimb movement in rats: the single pellet reaching test and staircase test. *Curr Protoc Neurosci*. 2012;58:8.28.1-8.28.15.
9. Alaverdashvili M, Whishaw IQ. A behavioral method for identifying recovery and compensation: hand use in a

Downloaded from nnr.sagepub.com at Scuola Superiore Sant'Anna on October 21, 2014

preclinical stroke model using the single pellet reaching task. *Neurosci Biobehav Rev*. 2013;37:950-967.
10. Whishaw IQ, Pellis SM, Gorny BP, Pellis VC. The impairments in reaching and the movements of compensation in rats with motor cortex lesions: an endpoint, videorecording, and movement notation analysis. *Behav Brain Res*. 1991;42:77-91.
11. Farr TD, Whishaw IQ. Quantitative and qualitative impairments in skilled reaching in the mouse (*Mus musculus*) after a focal motor cortex stroke. *Stroke*. 2002;33:1869-1875.
12. Whishaw IQ, Alaverdashvili M, Kolb B. The problem of relating plasticity and skilled reaching after motor cortex stroke in the rat. *Behav Brain Res*. 2008;192:124-136.
13. Whishaw IQ, Whishaw P, Gorny B. The structure of skilled forelimb reaching in the rat: a movement rating scale. *J Vis Exp*. 2008;18:e816.
14. Metz GA, Whishaw IQ. Skilled reaching an action pattern: stability in rat *(Rattus norvegicus)* grasping movements as a function of changing food pellet size. *Behav Brain Res*. 2000;116:111-122.
15. Whishaw IQ, Travis SG, Koppe SW, Sacrey LA, Gholamrezaei G, Gorny B. Hand shaping in the rat: conserved release and collection vs. flexible manipulation in overground walking, ladder rung walking, cylinder exploration, and skilled reaching. *Behav Brain Res*. 2010;206:21-31.
16. Alaverdashvili M, Leblond H, Rossignol S, Whishaw IQ. Cineradiographic (video X-ray) analysis of skilled reaching in a single pellet reaching task provides insight into relative contribution of body, head, oral, and forelimb movement in rats. *Behav Brain Res*. 2008;192:232-247.
17. Dominici N, Keller U, Vallery H, et al. Versatile robotic interface to evaluate, enable and train locomotion and balance after neuromotor disorders. *Nat Med*. 2012;18:1142-1149.
18. Braun RG, Andrews EM, Kartje GL. Kinematic analysis of motor recovery with human adult bone marrow-derived somatic cell therapy in a rat model of stroke. *Neurorehabil Neural Repair*. 2012;26:898-906.
19. Panarese A, Colombo R, Sterpi I, Pisano F, Micera S. Tracking motor improvement at the subtask level during robot-aided neurorehabilitation of stroke patients. *Neurorehabil Neural Repair*. 2012;26:822-833.
20. Rohrer B, Fasoli S, Krebs HI, et al. Movement smoothness changes during stroke recovery. *J Neurosci*. 2002;22:8297-8304.
21. Krebs HI, Krams M, Agrafiotis DK, et al. Robotic measurement of arm movements after stroke establishes biomarkers of motor recovery. *Stroke*. 2014;45:200-204.
22. Schroeter M, Jander S, Stoll G. Non-invasive induction of focal cerebral ischemia in mice by photothrombosis of cortical microvessels: characterization of inflammatory responses. *J Neurosci Methods*. 2002;117:43-49.
23. Schallert T, Fleming SM, Leasure JL, Tillerson JL, Bland ST. CNS plasticity and assessment of forelimb sensorimotor outcome in unilateral rat models of stroke, cortical ablation, parkinsonism and spinal cord injury. *Neuropharmacology*. 2000;39:777-787.
24. Baskin YK, Dietrich WD, Green EJ. Two effective behavioral tasks for evaluating sensorimotor dysfunction following traumatic brain injury in mice. *J Neurosci Methods*. 2003;129:87-93.
25. Clarkson AN, Huang BS, Macisaac SE, Mody I, Carmichael ST. Reducing excessive GABA-mediated tonic inhibition promotes functional recovery after stroke. *Nature*. 2010;468:305-309.
26. Spalletti C, Lai S, Mainardi M, et al. A robotic system for quantitative assessment and poststroke training of forelimb retraction in mice. *Neurorehabil Neural Repair*. 2014;28:169-178.
27. R Development Core Team. *R: A Language and Environment for Statistical Computing*. Vienna, Austria: R Foundation for Statistical Computing; 2008. http://www.R-project.org. Accessed January 9, 2014.
28. O'Bryant AJ, Allred RP, Maldonado MA, Cormack LK, Jones TA. Breeder and batch-dependent variability in the acquisition and performance of a motor skill in adult Long-Evans rats. *Behav Brain Res*. 2011;224:112-120.
29. Gholamrezaei G, Whishaw IQ. Individual differences in skilled reaching for food related to increased number of gestures: evidence for goal and habit learning of skilled reaching. *Behav Neurosci*. 2009;123:863-874.
30. Clarkson AN, Lopez-Valdes HE, Overman JJ, Charles AC, Brennan KC, Carmichael TS. Multimodal examination of structural and functional remapping in the mouse photothrombotic stroke model. *J Cereb Blood Flow Metab*. 2013;33:716-723.
31. Starkey ML, Bleul C, Maier IC, Schwab ME. Rehabilitative training following unilateral pyramidotomy in adult rats improves forelimb function in a non-task-specific way. *Exp Neurol*. 2011;232:81-89.
32. Guggenmos DJ, Azin M, Barbay S, et al. Restoration of function after brain damage using a neural prosthesis. *Proc Natl Acad Sci U S A*. 2013;114:21177-21182.

Downloaded from nnr.sagepub.com at Scuola Superiore Sant'Anna on October 21, 2014